This article has been accepted for publication in a future issue of this journal, but has not been fully edited. Content may change prior to final publication. Citation information: DOI 10.1109/JLT.2015.2414821, Journal of Lightwave Technology

In-fibre Bragg grating impact force transducer for studying head-helmet mechanical interaction in head impact

Robert C. Butz (B.Sc), and Christopher R. Dennison* (Ph.D.)

***Abstract*—In this work, we present the first Bragg grating based transducer system for application to trauma biomechanics, more specifically head-helmet contact force measurements secondary to headform impact. The transducer comprises an aluminum superstructure designed to withstand typical impact forces in helmeted impact and to have resonances that allow the overall sensor system to capture all relevant spectral components of force transients in impact. Structural finite element models and strain-optic relationships are used to predict transducer sensitivity to impact force as well as mechanical resonances. The model predictions are verified through experimental calibration, and calibration results are, on average, within 10% of model predictions of force sensitivity. The model predicted first mechanical resonance is 72 kHz. The impact force transducer is also validated for helmeted impacts using an industry standard impact experiment and test headform. Results indicate excellent repeatability: maximum standard deviation of force measurements of 0.4% of the net force applied to the impacted headform, and average error in the time duration of the force transients of only 4%. Transient impact forces measured with the Bragg grating transducer are in agreement with magnitudes inferred from work of previous researchers. The presented transducer can be applied with both helmet test and anthropomorphic headforms to measure distributions of transient forces and therefore hypotheses related to helmet performance and head injury.**

***Index Terms*—Bragg grating, optical fibre, force transducer, impact force, helmet, head injury, concussion, mild brain injury, skull fracture.**

I. Introduction

TRANSDUCERS based on in-fibre Bragg gratings (FBGs) [1] have been developed to measure a wide array of parameters including but not limited to strain [2][3], temperature [4], pressure [5], force [6][7], and refractive index [8]. The key attributes of FBGs that make them an enabling transducer for the above measurements are immunity to electro-magnetic interference, resistance to corrosive and humid environments, and in some cases the small size of FBGs (125 micron diameter and sensing gage lengths typically 1mm to 10mm) is attractive when compared to relatively larger transducers. The ability to serial-multiplex and apply them to distributed measurements has made FBGs an enabling technology for structural health monitoring [9] applications. In recent years, with advances in swept-laser light sources, high-bandwidth photo-detectors, and oscillating interferometric cavities, FBGs can be interrogated at rates from DC to kHz and are therefore suited to both static and dynamic measurements.

The desirable characteristics of FBGs and advances in interrogation techniques has led the author and many other researchers to develop transducers for a wide range of applications in science and engineering including, most relevant to the presented work, biomechanics [6], [10]–[12].

In the presented work, we focus on developing force transducers that measure transient forces resulting from head impact. This is the first application of FBGs to measurements in impact (trauma) biomechanics. As described subsequently, we exploit the characteristic of excellent frequency response and the capability to be multiplexed to develop a transducer that can be arrayed and applied in helmet and head injury research.

Finite element analysis (FEA) with skull-brain models has shown that transient focal impact forces on the skull lead to strain 'hot-spots' in the brain which initially form at the impact force site (coup site) and subsequently migrate through the brain as time progresses [13]. Because strain in brain tissue is thought to correlate with injury [14]–[16], these temporal hot-spot migrations could give insights into the underlying mechanisms of injury in terms of temporal head forces[17] and head kinematics [13]. The primary function of a helmet is to redistribute and limit forces on the head below fracture tolerances, increase the time-duration of these forces, limit peak head acceleration [18] and, thereby, shield the underlying bone and neurovascular structures from mechanical distress. The FEA work described above suggests that impact force location is a strong predictor of head injury risk. Therefore, measurement of impact location with corresponding temporal force distributions between the head and helmet could augment our understanding of helmet performance. Commercially available force sensing films have been applied,

Manuscript received November 27, 2014. This work was supported by the Natural Sciences and Engineering Research Council (Canada) Discovery Grants and Research Tools and Instruments programs as well as the Faculty of Engineering and Department of Mechanical Engineering at the University of Alberta.

Robert C. Butz is affiliated with the Department of Mechanical Engineering at the University of Alberta, Edmonton Alberta Canada T6G 2G8.

Christopher R. Dennison is the corresponding author and leads the Biomedical Instrumentation Lab of the Department of Mechanical Engineering, University of Alberta, Edmonton Alberta Canada T6G 2G8.

This article has been accepted for publication in a future issue of this journal, but has not been fully edited. Content may change prior to final publication. Citation information: DOI 10.1109/JLT.2015.2414821, Journal of Lightwave Technology

but on a very limited basis, and are subject to some key limitations.

Force sensitive films, including Prescale (Fuji Photo Film Co., Japan) and I-Scan (Flexiforce® and other variants, Tekscan Inc., Boston, MA) [19], [20] are the most common tools to measure contact force. Both are force-sensitive films inserted between the contacting surfaces under study. I-Scan can measure transient forces but Prescale only provides measures of peak force. Both have poor accuracy when applied to contoured surfaces (like the human head). The resulting error (14-28%) depends primarily upon film thickness and modulus, surface curvature, and the compressive modulus of the contacting materials [19], [20]. Force measurements with Prescale have been performed between helmet test headforms and hockey helmets. Results showed poor correlation between peak forces and injury risk [21], but, due to the limitations of Prescale, force durations and rates (temporal aspects of the impact) could not be determined. I-scan has been applied between helmet impact foam samples and metallic impactors and also with helmet test headforms [22], [23], but is subject to the significant measurement errors noted above. Notwithstanding these attempts to apply commercially available sensing technologies, there is currently no force transducer designed to integrate with helmet test headforms and measure transient forces relevant to helmet performance and head injury.

We present an FBG-based transient force transducer that can integrate with contoured surfaces of helmet test headforms. Strain-optic and linear elastic numerical modeling is used to determine force sensitivity and resonances. Calibration experiments are conducted to demonstrate that the force transducer is capable of resolving force transients and is repeatable in both the force-time and frequency domain. Validation experiments are conducted to demonstrate that the transducer is repeatable in helmeted impacts and that force measurements are in agreement with limited data found in the literature.

II. Materials and Methods

A. Design of impact force transducer

The impact force transducer comprises an FBG that is integrated into an aluminum superstructure. The superstructure is designed to withstand stresses created by transient impact forces that range up to 5kN, approximately double the typical range of expected impact forces in helmeted head impact (where skull fracture is almost non-existent) [24]. The superstructure is also designed to have mechanical resonances that are compatible with prevailing industry requirements for impact transducers as described subsequently.

Impact forces applied to the superstructure create strains in the superstructure and these force-dependent strains are transduced to optical wavelength shift using FBGs. FBGs are a permanent periodic variation in the refractive index of an optical fibre core [25]. The length of the FBG and the magnitude and spatial period of the variation in the refractive index determine the optical spectrum that is reflected from the FBG. When light spanning a broad range of wavelengths propagates in the core of a conventional single-mode fibre [26, p. 28] and encounters a Bragg grating, a narrow spectrum of wavelengths is reflected, centered at the Bragg wavelength:

$$\lambda_B = 2\Lambda n_0 \quad (1)$$

where Λ is the spatial-period of the variation in the refractive index and n_0 is the refractive index of the fibre core (1.468 at 1550 nm for Technica SA hydrogen loaded and degassed single-mode fibre, Technica SA, Beijing China).

Both mechanical strain and temperature perturbations at the grating will modulate (shift) the Bragg wavelength. The magnitude of Bragg wavelength shift is a function of the strain field and temperature over the region of the grating. In typical head-helmet impact scenarios, the timescale of impact forces ranges over 0 msec to 20 msec [18] and because these timescales are small relative to the timescale of ambient temperature fluctuations, we neglect thermal perturbations.

In the transducer presented in this work, forces (direction shown in Figure 1) induce mechanical strains in the aluminum superstructure, which are coupled into the FBG such that FBG strains are axial (along the axis of the fibre). For forces at right angles to the normal force (transverse forces) the Bragg grating is located near the neutral axis of the beam and therefore, from beam solid mechanics, there will be negligible strain at the beam's neutral axis and minimal strain coupled into the FBG. Moreover, the cross-sectional thickness of the beam is larger in the transverse direction (with respect to FBG orientation) and will result in lesser transverse-force induced strain than axial strains caused by normal forces. Because the axial strains are much greater, and the FBG is located at the neutral axis (transversely), there is minimal sensitivity to transverse forces. Changes in the Bragg wavelength, denoted by $\Delta\lambda_B$, proportional to the force-induced axial strain, ε, can be calculated as[25]:

$$\Delta\lambda_B = S_\varepsilon \varepsilon \quad (2)$$

where S_ε is the FBG sensitivity to axial strain (i.e. 1.2 pm/με [25]) that can be computed from the general tensorial notation used to predict strain sensitivity to strain fields.

The final transducer aluminum superstructure capable of withstanding 5kN impact forces has an outside diameter of 12mm and thickness of 3mm (Figure 1). A threaded hole is centrally located and on opposing sides of this hole are two parallel channels (nominal length 5mm, depth 2mm). The purpose of the hole is to provide an alignment and fixation point for sensor manufacture. The lengths of the channels define the length of a fixed-fixed mechanical beam (Figure 1) which deforms when impact forces are transmitted onto the transducer. In the present sensor configuration, a single FBG is permanently fixed to the underside of the beam (Epoxy 907, Miller Stephenson Chemical Company Inc., Danbury CT), nominally 2.5 mm from the center of the threaded hole. This surface-mounted FBG experiences strain when the fixed-fixed beam deforms. These strains are directly proportional to beam deflection, which is in turn directly proportional to impact force. The fibre containing the FBG is strain-relieved via a rigid epoxy-aluminum-fibre junction where the fibre that supplies light to the FBG enters the superstructure (Figure 1). The Bragg gratings used in this work (Technica SA, Beijing

This article has been accepted for publication in a future issue of this journal, but has not been fully edited. Content may change prior to final publication. Citation information: DOI 10.1109/JLT.2015.2414821, Journal of Lightwave Technology

China) were centered at nominally 1550 nanometers (nm), were 1mm long, had a nominal full-width at half maximum of 1.5nm, and had nominal reflectivity of 60% in single mode fibre (SMF-28C).

B. Sensor analysis

The finite-element method, implemented using ABAQUS Explicit (version 6.12, Dassault Systems Simulia Corp., Providence, RI), was used to analyze the sensor for both force sensitivity and mechanical resonances (modal analysis). A structural model comprising ABAQUS HEX elements (8-node linear brick) was created to match the physical dimensions of the transducer in Figure 1. The model comprised both the aluminum (6061-T6, Young's Modulus = 68.9 GPa, Poisson's Ratio = 0.33 [27]) superstructure and the optical fibre (125 micron diameter, Young's Modulus = 69 GPa, Poisson's Ratio = 0.17, [25] as shown in Figure 1). The contact between the optical fibre and aluminum was modeled as a tie constraint, which eliminates the degrees of freedom on adjacent nodes on the aluminum and optical fibre and couples the motion of the fibre nodes to the motion of the aluminum.

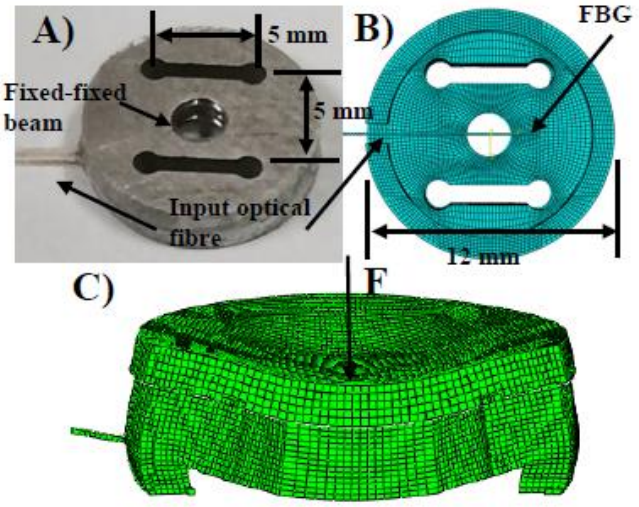

Figure 1: Prototype impact force transducer. A. External view of transducer with the FBG fixed to underside of the fixed-fixed beam. B. Finite-element model of underside view of transducer. C. Deformation of transducer under impact loading.

Initially, tetrahedral elements comprised the model and were used to assess convergence. The criterion for convergence was that, for increasing number of elements and for an applied force of 1200 N, peak principal strain magnitude changed less than 10% of the previous peak strain magnitude. Once the number of tetrahedral elements based on this criterion was established, the element topology was changed to triangular and peak strains were again solved to ensure that strains were invariant based on element type (<10% change). The outcome of this procedure resulted in the final structural model with 57,053 HEX tetrahedrons.

To ascertain force sensitivity, forces were modeled to increase from 0 N to 1200 N in 100 N increments and the strain at the FBG location was solved at each load increment. The FBG strain was then input to Equation 2 to determine the corresponding shift in Bragg wavelength. The outcome of this procedure was model-predicted Bragg wavelength shift as a function of applied load, allowing expression of force sensitivity in units of Newtons per nm of wavelength shift (N/nm).

To ascertain mechanical resonances of the transducer, a modal analysis was performed. The purpose of this analysis was to confirm that the first (lowest) resonance exceeded the requirements on mechanical resonance of helmet and crash-test headforms (no resonances can exist below 2,000 Hz [28]) and in so doing, confirm that mechanical resonances of the headform will not induce resonance (and therefore measurement error) in the impact force transducer.

C. Sensor calibration

Three impact force transducers were constructed and calibrated as shown in Figure 2. The calibration apparatus included a falling impacter (5 kg total mass) at the mass-center of which was a piezo-electric accelerometer (Neill-Tech, Xiamen Niell Electronics Co., China, 2,000g range) with frequency response typical of industry standards for crash and helmet testing [29]. The Bragg grating impact force transducer was fixed to a metal anvil (AISI 4130 Steel, 161 kg mass), and positioned below the impacter (Figure 2). A compliant neoprene rubber (durometer of 70A, thickness of 1.6 mm) layer was placed on the impact sensing surface of the transducer and this neoprene served the dual purpose of limiting impacter acceleration to that typical of helmeted impact (range 10 g-forces or "g" to 200 g) and creating an appropriate time-duration of impact force that matched that typical of helmeted impacts (range 5 msec to 20 msec). The drop distance between the impacter and force transducer (1 cm) was set to create peak impact force magnitude of 2 kN, which brackets a realistic range of impact forces that could be experienced by a helmeted head that does not suffer skull fracture.

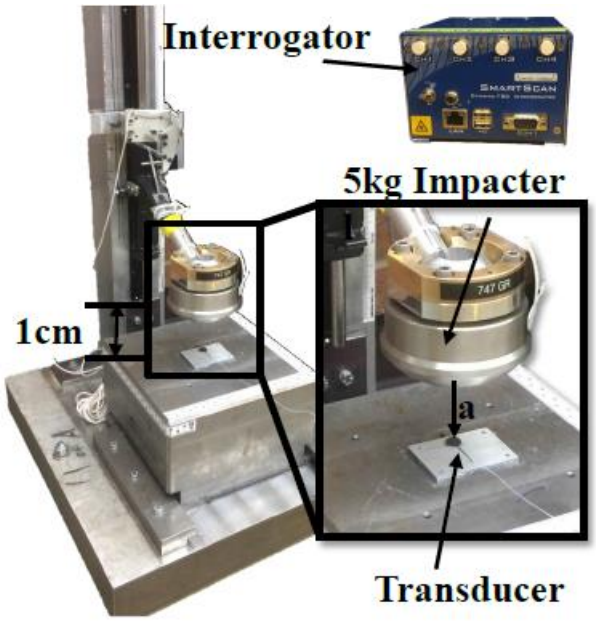

Figure 2: Calibration apparatus. (Inset) Impacter set 1 cm above the impact transducer. The Bragg grating interrogator is also shown.

This article has been accepted for publication in a future issue of this journal, but has not been fully edited. Content may change prior to final publication. Citation information: DOI 10.1109/JLT.2015.2414821, Journal of Lightwave Technology

Analog voltages from the accelerometer were interrogated at 100 kHz and were anti-alias filtered and subsequently low-pass filtered at a cutoff frequency of 1650 Hz in accordance with industry standards for impact telemetry [29]. Analog voltages were measured using National Instruments hardware (PXI 6251, National Instruments, Austin, TX) and software (LabVIEW, version 8.5, National Instruments, Austin, TX). Wavelength shifts from the FBG force transducer were acquired at 10 kHz using a commercially available interrogator (SmartScan, Smart Fibres Ltd., UK, 25 kHz bandwidth, 4 channel). Like the acceleration data, impact induced wavelength shifts were low-pass filtered in accordance with industry standards for impact telemetry.

Following calibration experiments, all acceleration and wavelength data were synchronized in time (with the filtered accelerations down sampled to 10 kHz). Impact force was computed from acceleration data by multiplying the measured impacter acceleration by the total falling mass of the impacter. The synchronized impact force and impact wavelength data were then plotted and simple linear regression was performed to compute impact transducer sensitivity (N/nm) and the coefficient of determination of the linear fit. Each impact force transducer was calibrated 3 times. A discrete Fourier transform was also performed to both the acceleration and wavelength data. The DFT allows comparison of spectral characteristics or, in other words, to confirm that the impact force transducer records all frequencies that the industry standard accelerometer records and therefore that no important frequency harmonics are missed.

D. Sensor integration with Magnesium helmet test headform

The impact force transducers were integrated with a magnesium helmet test headform (size medium, mass = 2,511.7 g, circumference = 575 mm, CADEX Inc., St-Jean-sur-Richelieu, QC, Canada) to allow an assessment of sensor repeatability and to compare measurements from the transducer presented here and the limited measurements found in previous literature. The magnesium headform was retrofit with a custom made impact resistant acrylic cover (3.5 mm thickness) and a retainer hole was created in the acrylic cover at the headform apex (Figure 3) to retain the impact force transducers. The impact transducer was set into the acrylic, with a neoprene rubber cover, such that the top surface of the neoprene was less than 1mm above the acrylic. The magnesium headform was then installed on a linear drop rail (total falling mass of 4.7 kg, Figure 3) and a commercially available hockey helmet (Bauer model HH1000S, size 520 – 570 mm) was fit onto the head.

The helmeted headform was subjected to linear impacts at heights of 0.5 m, 1.0 m and 1.5 m and the configuration of the impact experiment was in conformance with the certification standard of contemporary hockey helmets (ASTM F1045) [30]: helmet impact onto steel anvil covered with an elastomer pad of thickness of 1 inch and shore A hardness of 60 ± 2 (CADEX Inc., St-Jean-sur-Richelieu, QC, Canada). Headform accelerations and impact transducer wavelength shifts were measured using the same techniques as those described for sensor calibration. Five impacts were conducted at each drop height.

III. RESULTS

A. Numerical predictions of force sensitivity and resonance

The combined ABAQUS structural and strain-optic model predicts a direct linear relationship between impact force and Bragg wavelength shift (Figure 4). The model predicted a sensitivity to force of 873.94 N/nm and a least-squares fit of the model data indicated coefficient of determination of 1.0 (Figure 4).

The ABAQUS simulations predicted first mechanical resonance at approximately 72 kHz. The deformation associated with the first mode resonance is inset in Figure 4 and can be qualitatively described as that of the first mode of a fixed-fixed mechanical beam.

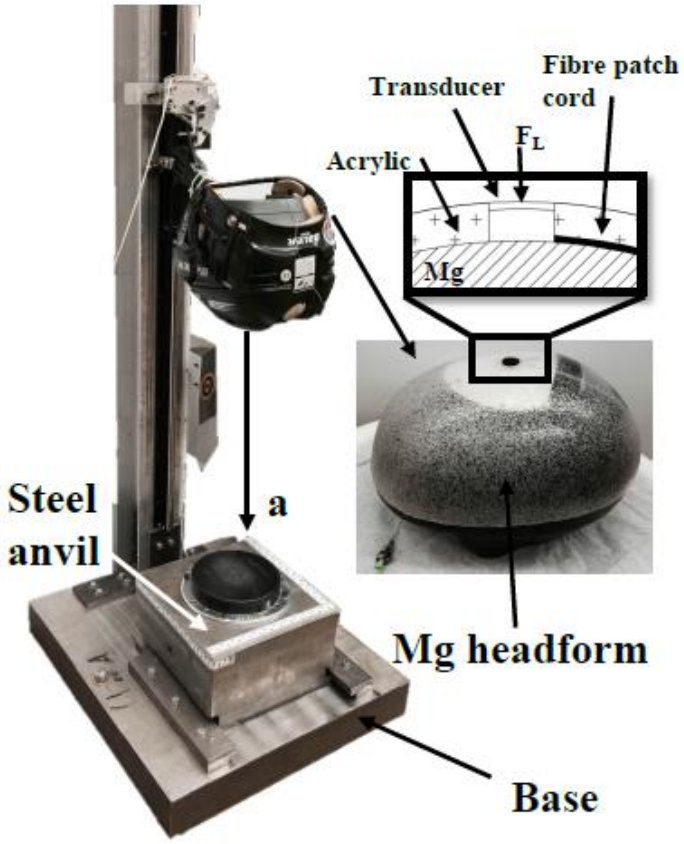

Figure 3: Experimental configuration used to assess repeatability of impact force transducers in helmeted impact. As shown (inset) an impact resistant acrylic skin (3.5 mm nominal thickness) with a conformal fit to the magnesium headform retains the sensor near the apex of the headform. The headform is installed on a linear drop experiment, and a hockey helmet is placed over the headform.

This article has been accepted for publication in a future issue of this journal, but has not been fully edited. Content may change prior to final publication. Citation information: DOI 10.1109/JLT.2015.2414821, Journal of Lightwave Technology

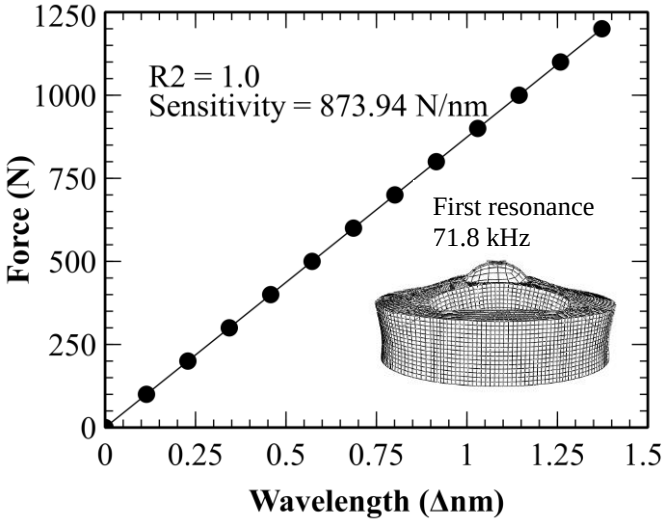

Figure 4: ABAQUS-strain-optic predicted linear relationship between impact force and Bragg wavelength shift.

B. Calibration for impact force transduction

Figure 5 shows typical characteristic force (calculated from accelerometer) versus time as well as impact-induced Bragg wavelength shift from the impact transducer, versus time. The mean time duration of the measured acceleration pulse (Δt) for the accelerometer, transducer 1, transducer 2 and transducer 3 are 4.6 msec, 5.1 msec, 5.0 msec and 5.2 msec, respectively. The mean differences between the accelerometer Δt and those of the impact transducers are 9%, 8% and 11% for transducer 1, transducer 2 and transducer 3, respectively.

Figure 6 shows typical impact force versus impact-induced wavelength shift characteristics for the three transducers. Sensitivities to force were calculated using the mean sensitivity for each transducer over three calibration trials. As shown, data for all three transducers exhibits linearity over the range of impact forces. The mean calculated slope, or sensitivity to force, is 1198.9 N/nm for transducer 1, 521.9 N/nm for transducer 2 and 635.5 N/nm for transducer 3. The mean coefficients of determination (R^2) are > 0.95 for all three transducers (Figure 6).

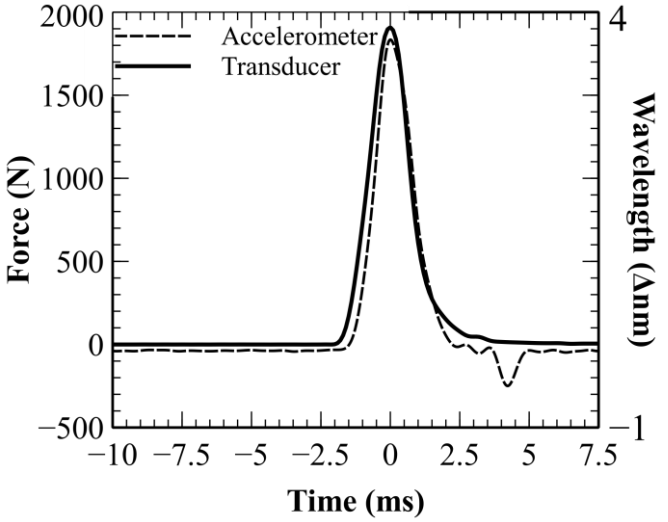

Figure 5: Typical impact force applied to the impact transducer (solid line, calculated from accelerometer signal) and impact-induced wavelength shift (dashed line). Solid line is a locus through data collected at 100 kHz. Dashed line is the locus through wavelength data collected at 10 kHz. Presented data is low-pass filtered at 1650 Hz corner frequency. Data is for Transducer 2.

The mean sensitivity to force for all three transducers (785.4 N/nm) is 10% lower than the predicted sensitivity from the ABAQUS structural and strain-optic model.

Table 1 shows both the experimental sensitivities to force and the coefficients of determination for each force transducer. As stated above the experimental sensitivities for each transducer is a linear relationship (mean $R^2 > 0.95$) between impact force and impact-induced wavelength shift.

Figure 7 shows typical spectral results from discrete Fourier transform of force measurements from both the accelerometer and three datasets from the impact force transducers. As shown, the accelerometer and force transducers do not register significant harmonics past approximately 250 Hz and the general characteristic shape of the Fourier amplitude versus frequency characteristic is the same between accelerometer and force transducers. Also of note, the impact force transducers do not appear to resonate when subjected to impact forces at timescales typical of helmet impact (as indicated by nominally zero amplitude beyond 250 Hz).

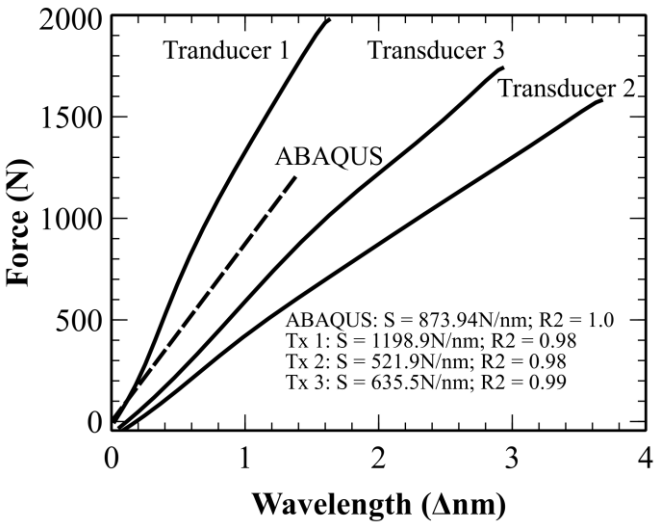

Figure 6: Typical calibration characteristics for three prototypes constructed. Data presented is low-pass filtered.

TABLE I

The sensitivity of each impact transducer and the corresponding coefficient of determination. Each transducer was calibrated three times and the mean sensitivity to force for each transducer can be found in Figure 6. All sensitivities reported in units of Newtons per nm of wavelength shift (N/nm).

	Sensitivity (N/nm)	**R^2**	
Transducer 1	1198.9	0.98	**Mean**
	61.6	0.019	**Std. Dev**
	1118.5 - 1268.1	0.95 - 0.99	**Range**
Transducer 2	442.9	0.98	**Mean**
	7.8	0.017	**Std. Dev**
	431.9 - 448.6	0.95 - 0.99	**Range**
Transducer 3	516.6	0.99	**Mean**
	13.0	0.0047	**Std. Dev**
	502.2 - 533.7	0.98 - 0.99	**Range**

This article has been accepted for publication in a future issue of this journal, but has not been fully edited. Content may change prior to final publication. Citation information: DOI 10.1109/JLT.2015.2414821, Journal of Lightwave Technology

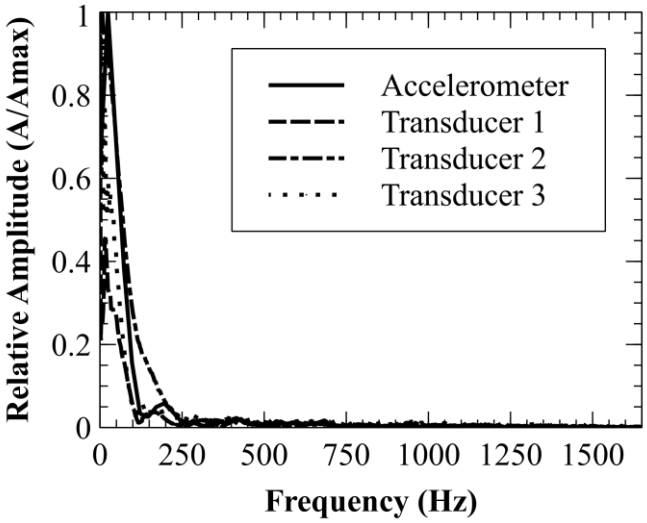

Figure 7: Spectral results from discrete Fourier transform of force measurements of a helmeted impact at a drop height of 0.5 m from both the accelerometer and three impact force transducers. Cutoff frequency is 1650 Hz.

C. Validation of sensors in magnesium headform

Figure 8 shows the typical net head force (calculated from accelerometer and using the total falling mass of 4.7 kg, left axis) versus time as well as local impact force from the impact transducer (measured with transducer 2, right axis), versus time. The typical net head force and local impact force were obtained at incremental drop heights of 0.5 m, 1.0 m and 1.5 m. Each trace has been artificially shifted to allow efficient presentation of all results in a single figure. The measured net head force is 3352.7 N for a 0.5 m drop height, 7005.3 N for a 1.0 m drop height and 11054 N for a 1.5 m drop height. The local impact force is 78 N for a 0.5 m drop height, 163 N for a 1.0 m drop height and 260 N for a 1.5 m drop height (Figure 8).

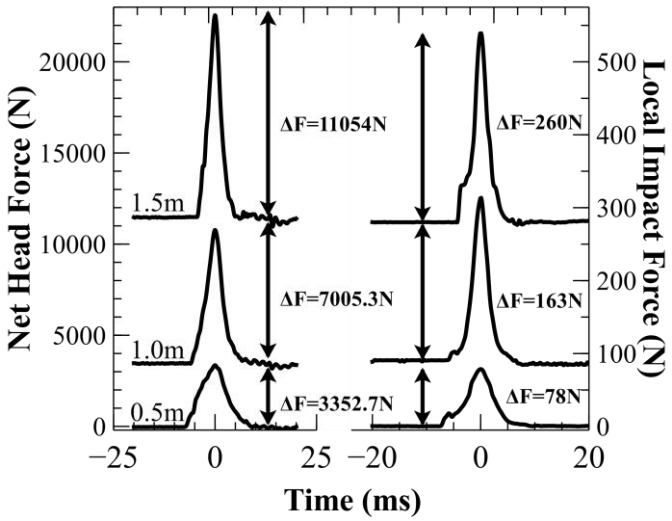

Figure 8: Typical net head force (left) and local impact force (right) from three headform drop heights (0.5m, 1.0m, and 1.5m).

Figure 9 shows the mean and first standard deviation of local impact force measurements for each force transducer. The mean local impact force for transducer 1 is 73.2 N for a 0.5 m drop height, 165.9 N for a 1.0 m drop height and 211.6 N for a 1.5 m drop height. The first standard deviation for transducer 1 at a drop height of 0.5 m, 1.0 m and 1.5 m is 0.8 N, 9.5 N and 13.1 N, respectively. The mean local impact force for transducer 2 is 71.6 N for a 0.5 m drop height, 170.0 N for a 1.0 m drop height and 256.3 N for a 1.5 m drop height. The first standard deviation for transducer 2 at a drop height of 0.5 m, 1.0 m and 1.5 m is 8.8 N, 29.5 N and 6.3 N, respectively. The mean local impact force for transducer 3 is 55.4 N for a 0.5 m drop height, 150.5 N for a 1.0 m drop height and 262.5 N for a 1.5 m drop height. The first standard deviation for transducer 3 at a drop height of 0.5 m, 1.0 m and 1.5 m is 3.1 N, 26.3 N and 16.1 N, respectively.

Table 2 shows the net head force (F_N) and local impact force (F_L) for each validation drop. The mean percentage ± standard deviation of net head force captured by transducer 1, transducer 2 and transducer 3 is 2.24 ± 0.2%, 2.30 ± 0.3% and 2.17 ± 0.4%, respectively.

Table 3 shows the time duration of impact pulse (defined as time between first increase from pre-impact force and time at which measured force returns to pre-impact magnitude) measured using the accelerometer (Δt_a) and impact transducer (Δt_t) for the helmeted impacts. The mean difference in time duration between the accelerometer and transducer 1, transducer 2 and transducer 3 is 0.93 msec, 0.69 msec and 0.57 msec, respectively.

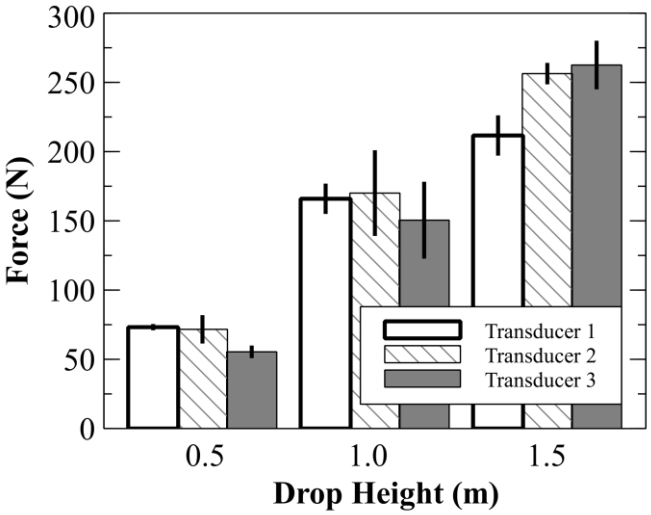

Figure 9: Mean and first standard deviation of impact force measurements for the three prototypes constructed.

TABLE II

The net head force (F_N) and local impact force (F_L) at incremental drop heights of 0.5 m, 1.0 m and 1.5 m. Five trials were performed at each drop height and the mean force measurements are shown in Figure 9. All forces reported in units of Newtons (N). The mean value (Top value), standard deviation (middle value), and range of values (bottom value) are presented in the table.

	0.5 m		1.0 m		1.5 m	
Transducer	F_N*	F_L*	F_N*	F_L*	F_N*	F_L*
1						
Mean	3032.8	73.2	7094.4	165.9	10707.9	211.6
Std. Dev	26.8	0.8	173.4	9.5	412.1	13.1

This article has been accepted for publication in a future issue of this journal, but has not been fully edited. Content may change prior to final publication. Citation information: DOI 10.1109/JLT.2015.2414821, Journal of Lightwave Technology

Range	3004.1 to 30673.4	71.8 to 74.3	6914.6 to 7305.9	157.3 to 182.9	9979.3 to 11164	191 to 232.4
2						
Mean	3296.0	71.6	7022.8	170.0	11051.4	256.3
Std. Dev	45.9	8.8	133.5	29.5	222.7	6.3
Range	3213.2 to 3352.7	54.4 to 78.7	6901.4 to 7276.0	161.2 to 224	10665 to 11321	247.9 to 265.7
3						
Mean	3270.4	55.4	6647.1	150.5	10279.9	262.5
Std. Dev	72.7	3.1	200.4	26.3	384.1	16.1
Range	3195.6 to 3392.3	51.8 to 60.7	6358.3 to 6869.9	117.2 to 182.7	9654.7 to 10812	260.0 to 289.0

* units (N)

TABLE III

The time duration of helmeted impact for both the accelerometer (Δt_a) and each transducer (Δt_t) at incremental drop heights of 0.5 m, 1.0 m and 1.5 m. Five trials were performed at each drop height. All time durations reported in units of milliseconds (msec). The mean value (Top value), stamdard deviation (middle value), and range of values (bottom value) are presented in the table.

	0.5 m		1.0 m		1.5 m	
Transducer	Δt_a*	Δt_t*	Δt_a*	Δt_t*	Δt_a*	Δt_t*
1						
Mean	17.1	15.7	15.0	14.4	10.4	10.0
Std. Dev	0.3	0.4	1.3	0.9	0.4	0.5
Range	16.7 to 17.5	15.1 to 16.2	13.4 to 16.8	12.8 to 15.6	9.8 to 11.0	9.4 to 10.8
2						
Mean	16.2	15.3	15.3	14.5	9.9	9.7
Std. Dev	0.8	0.6	1.4	0.9	0.5	0.6
Range	14.6 to 17.0	14.4 to 16.2	13.2 to 16.8	13.7 to 15.8	9.0 to 10.5	8.8 to 10.4
3						
Mean	17.1	16.7	14.0	13.5	10.5	10.6
Std. Dev	0.3	1.2	1.1	0.9	0.2	0.1
Range	16.5 to 17.4	15.2 to 18.8	13.2 to 16.1	12.9 to 15.3	10.3 to 11.0	10.5 to 10.8

* units (msec)

IV. Discussion

We have developed an FBG-based impact force transducer for application in injury (trauma) biomechanics and for the presented work specifically, impact force transduction during helmeted head impact. The impact force transducer measures contact forces between helmet liners and the helmet test headform. The calibration results presented indicate that the transducer captures transient force signals that are characteristic of helmeted head impact and is repeatable. To our knowledge, this is the only FBG-based impact transducer for applications in trauma biomechanics. Moreover, the presented transducer is able to integrate with anthropomorphic and helmet test headforms and have transient performance exceeding industry standards on frequency and mechanical resonance. Also, the presented transducer does not suffer from measurement errors associated film curvature with existing applied commercially available force sensitive films.

Calibration results exhibit repeatability and linearity over the force range of interest and further convey that the spectral characteristics of the impact force transducer are appropriate for studying helmeted impact. Calibration results (Table I) indicate that a linear fit to calibration data is appropriate (majority of R^2 0.98 or greater) and that the variance in calibration results (slope) is 5% or less for all transducers calibrated. More specifically, the first standard deviation in the calibration sensitivity is 5%, 2% and 3% of the mean sensitivity for transducer 1, 2 and 3, respectively. The results from the spectral analysis of accelerometer and force transducer data (Figure 7) indicate that the transducer registers harmonics at 250 Hz or less, in complete agreement with results reported from the industry-standard accelerometers used for crash and helmet testing to which we compare. Overall, these calibration and spectral results are in agreement with ABAQUS-strain optic predictions of sensitivity and resonance. We acknowledge that there is considerable variation in inter-sensor sensitivity (Table I), but these differences owe mainly to minor differences in transducer fabrication. Bragg grating location on the superstructure varies slightly between transducers and, as a result, the strain transferred to the grating for a given force will also vary. Because the amount of strain coupled into the grating varies based on minor differences in grating location (each transducer will have slightly different Bragg grating location) sensor sensitivity varies. It is worth noting, however, that on average the experimental sensitivity of our collection of transducers is only 10% lower than the model predicted. Furthermore, as described below, the variation in the inter-sensor sensitivity did not affect the overall validation of the transducers in helmeted impact.

In measurements of local force during helmeted impact, the impact force transducers exhibit repeatability in both the force and time domain and this is a positive result in the context of future application of studying injury risk associated with force transients. In the context of predicting risk of head/brain injury in helmeted impact, the critical telemetry required to calculate the majority of existing injury risk assessment functions are acceleration magnitude versus time and acceleration duration [16]. In the context of the brain finite element studies cited in the introduction, it will be critical that accurate depictions of force transients can be measured. Our validation results convey that each transducer repeatedly captured 2% of the net head force and the standard deviation in these measurements was negligible (0.2%, 0.3% and 0.4% for transducers 1 through 3, respectively). Furthermore, the measured timescale

This article has been accepted for publication in a future issue of this journal, but has not been fully edited. Content may change prior to final publication. Citation information: DOI 10.1109/JLT.2015.2414821, Journal of Lightwave Technology

of the force transients was in excellent agreement with acceleration measures (Table III). The average difference in Δt between the accelerometers and force transducers was 0.6 msec (4% of mean Δt measured by the industry standard accelerometer). Taken together, these results suggest that when an array of impact force transducers is distributed over a headform, the transducers will give repeatable measurements of transient force distributions.

The force magnitudes measured using the impact transducers presented in this work are comparable to previously published data for helmeted impacts using ASTM certified hockey helmets. In novel work from Ouckama et al. [22] peak helmet-head contact forces as measured with a variant of TekScan© are presented (average velocity of 4.5 m/s, which corresponds to a drop height of 1 m). For similar helmets with vinyl-nitrile impact liner dropped from 1m, the mean force magnitudes measured using the impact transducers presented in our work is 162.2 N, which is 12.3% higher than the force magnitude presented by Ouckama et al. (2012) of 144.4 N (rear helmet impacts). Care must be taken in comparing these results because the location of our transducers (head apex) is different than the location to which we compare (rear in Ouckama et al.). Nevertheless, the results from the presented transducers are comparable, and we further note that for frontal helmet impacts, Ouckama et al. report peak force of 136.6 N (15.8% lower than 162.2 N). Impacts to the helmet rear and helmet front zones could be seen as similar to impacts to the apex because the amount of impact liner compressed in these impacts would be similar.

Like any experimental study, the presented work has limitations. Our impact force transducer was validated at a single location on the magnesium headform and this single location validation could be seen as incomplete. Given the high degree of repeatability exemplified in our results, and the agreement between our measurements and those of other research groups, we feel that the results in this work are promising. Furthermore, there is no a priori reason to believe that the impact transducer would have head-location dependent repeatability, but with continued use in our ongoing program we will repeatedly quantify and verify our results against the work of others.

The methods presented to validate the impact force transducer required that an impact resistant acrylic cover be integrated with the headform. The decision to retain the sensors using the cover was made primarily to avoid making permanent changes to the magnesium headform which would invalidate the headform certification, making it unusable for helmet performance testing against certification standards (eg. ASTM, CSA). The purpose of the acrylic cover is to insure that the force sensing surface and the rest of the head are continuous, but the presence of an acrylic cover is not a requirement for application of the impact transducer. Our long term plans for the impact transducers presented here are to integrate them into dedicated magnesium and subsequently other anthropomorphic headforms, purpose-machined to house the force transducers, which will be dedicated to research projects requiring measurement of head force transients.

Notwithstanding the limitations above, the presented work has strengths relative to the work of others. Standards for impact instrumentation used in helmet certification (and also applied in helmet research) have strict requirements on frequency response of instrumentation (accelerometers in the case of helmets) that ensure that all harmonics in measured signals can be successfully reproduced and compared between laboratories. Therefore, it is critical that any impact force transducer match the spectral performance of the accelerometers used for helmet certification. The Fourier analysis of our transducer results (Figure 7) indicates agreement with the spectral distribution of the accelerometer when calibrated *and* when applied on the headform. Spectral considerations are lacking in the results which have been reported using TekScan© [22], [23] films and therefore it is unclear whether these films measure all important harmonics in the presented impacts on the headform.

The results from our impact transducer, in terms of inter-test variance in peak measured force, compare well that that presented for previous attempts with TekScan© [22], [23]. For example, in Ouckama's novel work, the maximum apparent standard deviation (two standard deviations as indicated by error bars) in peak local force measurements is approximately 200N (for a similar vinyl nitrile helmet at 1m drop height) while for our results the maximum standard deviation was 59 N (Figure 9, Transducer 2, 1m drop height).

In this work, we have developed an FBG-based impact force transducer and demonstrated its repeatability in both the force-time and frequency domain for helmeted impacts. The sensor is readily applied with existing Bragg grating interrogators, allowing arrays of force transducers to be deployed on helmet test and anthropomorphic test headforms that are commonly used today to study helmet performance and hypothesis on head injury.

ACKNOWLEDGMENT

The authors wish to acknowledge support from the Natural Sciences and Engineering Research Council (NSERC) of Canada, and The Faculty of Engineering and Department of Mechanical Engineering at the University of Alberta. We also wish to thank Mr. Henry Yu for his contribution to commissioning the impact experiment and optical equipment.

REFERENCES

[1] K. O. Hill and G. Meltz, "Fiber Bragg grating technology fundamentals and overview," *J. Light. Technol.*, vol. 15, pp. 1263–1276, 1997.

[2] D. C. Betz, G. Thursby, B. Culshaw, and W. J. Staszewski, "Advanced layout of a fiber Bragg grating strain gauge rosette," *J. Light. Technol.*, vol. 24, no. 2, pp. 1019–1026, Feb. 2006.

[3] M. S. Muller, T. C. Buck, H. J. El-Khozondar, and A. W. Koch, "Shear Strain Influence on Fiber Bragg Grating Measurement Systems," *J. Light. Technol.*, vol. 27, no. 23, pp. 5223–5229, Dec. 2009.

[4] W. Qiu, X. Cheng, Y. Luo, Q. Zhang, and B. Zhu, "Simultaneous Measurement of Temperature and Strain

Using a Single Bragg Grating in a Few-Mode Polymer Optical Fiber," *J. Light. Technol.*, vol. 31, no. 14, pp. 2419–2425, Jul. 2013.

[5] D. A. Singlehurst, C. R. Dennison, and P. M. Wild, "A Distributed Pressure Measurement System Comprising Multiplexed In-Fibre Bragg Gratings Within a Flexible Superstructure," *IEEE J. Light. Technol.*, vol. 30, pp. 123–129, 2012.

[6] C. R. Dennison, P. M. Wild, D. R. Wilson, and M. K. Gilbart, "An in-fiber Bragg grating sensor for contact force and stress measurements in articular joints," *Meas. Sci. Technol.*, vol. 21, p. 115803, 2010.

[7] S. Li-Yang, J. Qi, and A. Jacques, "Fiber optic pressure sensing with conforming elastomers," *Appl. Opt.*, vol. 49, pp. 6784–6788, 2010.

[8] S.-M. Lee, M.-Y. Jeong, and S. S. Saini, "Etched-Core Fiber Bragg Grating Sensors Integrated With Microfluidic Channels," *J. Light. Technol.*, vol. 30, no. 8, pp. 1025–1031, Apr. 2012.

[9] S. Javdani, M. Fabian, M. Ams, J. Carlton, T. Sun, and K. T. V. Grattan, "Fiber Bragg Grating-Based System for 2-D Analysis of Vibrational Modes of a Steel Propeller Blade," *J. Light. Technol.*, vol. 32, no. 23, pp. 3991–3997, Dec. 2014.

[10] C. R. Dennison, P. M. Wild, P. W. G. Byrnes, A. Saari, E. Itshayek, D. C. Wilson, Q. A. Zhu, M. F. S. Dvorak, P. A. Cripton, and D. R. Wilson, "Ex vivo measurement of lumbar intervertebral disc pressure using fibre-Bragg gratings," *J. Biomech.*, vol. 41, pp. 221–225, 2008.

[11] L. Mohanty, S. C. Tjin, D. T. T. Lie, S. E. C. Panganiban, and P. K. H. Chow, "Fiber grating sensor for pressure mapping during total knee arthroplasty," *Sens. Actuators A*, vol. 135, pp. 323–328, 2007.

[12] L. Carvalho, J. C. C. Silva, R. N. Nogueira, J. L. Pinto, H. L. Kalinowski, and J. A. Simoes, "Application of Bragg grating sensors in dental biomechanics," *J. Strain Anal.*, vol. 41, pp. 411–416, 2006.

[13] D. C. Viano, I. R. Casson, E. J. Pellman, L. Zhang, A. I. King, and K. H. Yang, "Concussion in professional football: brain responses by finite element analysis: part 9," *Neurosurgery*, vol. 57, no. 5, pp. 891–916; discussion 891–916, Nov. 2005.

[14] W. N. Hardy, M. J. Mason, C. D. Foster, C. S. Shah, J. M. Kopacz, K. H. Yang, A. I. King, J. Bishop, M. Bey, W. Anderst, and S. Tashman, "A Study of the Response of the Human Cadaver Head to Impact," *Stapp Car Crash J. Vol 51*, vol. 51, pp. 17–80, 2007.

[15] A. I. King, "Fundamentals of impact biomechanics: Part I--Biomechanics of the head, neck, and thorax," *Annu Rev Biomed Eng*, vol. 2, pp. 55–81, 2000.

[16] D. Marjoux, D. Baumgartner, C. Deck, and R. Willinger, "Head injury prediction capability of the HIC, HIP, SIMon and ULP criteria," *Accid. Anal. Prev.*, vol. 40, no. 3, pp. 1135–1148, Dec. 2007.

[17] L. Zhang, K. H. Yang, and A. I. King, "Comparison of brain responses between frontal and lateral impacts by finite element modeling," *J. Neurotrauma*, vol. 18, no. 1, pp. 21–30, Jan. 2001.

[18] J. A. Newman, "Biomechanics of Head Trauma: Head Protection," in *Accidental Injury: Biomechanics and Prevention*, New York, USA: Springer Verlag, 2002, pp. 303–323.

[19] J. Z. Wu, W. Herzog, and M. Epstein, "Effects of inserting a pressensor film into articular joints on the actual contact mechanics," *J. Biomech. Eng.*, vol. 120, pp. 655–659, 1998.

[20] D. R. Wilson, M. V. Apreleva, M. J. Eichler, and F. R. Harrold, "Accuracy and repeatability of a pressure measurement system in the patellofemoral joint," *J. Biomech.*, vol. 36, pp. 1909–1915, 2003.

[21] C. R. Castaldi and E. F. Hoerner, *Safety in Ice Hockey*. ASTM International, 2003.

[22] R. Ouckama and D. J. Pearsall, "Evaluation of a flexible force sensor for measurement of helmet foam impact performance," *J. Biomech.*, vol. 44, no. 5, pp. 904–909, Mar. 2011.

[23] R. Ouckama and D. J. Pearsall, "Impact performance of ice hockey helmets: head acceleration versus focal force dispersion," *Proc. Inst. Mech. Eng. Part P J. Sports Eng. Technol.*, vol. 226, no. 3–4, pp. 185–192, 2012.

[24] N. Yoganandan and F. A. Pintar, "Biomechanics of temporo-parietal skull fracture," *Clin. Biomech. Bristol Avon*, vol. 19, no. 3, pp. 225–239, Mar. 2004.

[25] R. M. Measures, *Structural Health Monitoring with Fiber Optic Technology*, vol. 1st. Academic Press, 2001.

[26] "Corning SMF-28 optical fibre: Product Information," *Corning Inc. Midl. MI Wwwcorningcomopticalfibre*, 2001.

[27] R. L. Norton, *Machine Design, An integrated approach*, 2nd ed. Prentice Hall, 2000.

[28] "EN 960:2006 Headforms for use in the testing of protective helmets." European Committee for Standardization (CEN).

[29] S. of A. Engineers, "J211 - (R) Instrumentation for impact test - Part 1 - electronic instrumentation," Society of Automotive Engineers, 2003.

[30] "ASTM F1045-07: Standard Performance Specification for Ice Hockey Helmets." .